Journal of the Association of Arab Universities for Basic and Applied Sciences (2013) **14**, 32–37

University of Bahrain

Journal of the Association of Arab Universities for Basic and Applied Sciences

www.elsevier.com/locate/jaaubas
www.sciencedirect.com

تحليل التشتت المرن للبيونات المشحونة عن نواة كالسيوم-40 في منطقة الطاقة المتوسطة

زهير شحادة [1،2]

[1] دائرة الفيزياء، جامعة الطائف، الطائف، المملكة العربية السعودية

[2] باحث زائر، قسم الفيزياء، جامعة جنوب الينوي، الولايات المتحدة الأمريكية

الملخص:

النتائج التجريبية للمقاطع المستعرضة التفاضلية للتشتت المرن للبيونات المشحونة عن نواة كالسيوم–40 تم تحليلها باستخدام جهد ضوئي موضعي بسيط لـ 50، 65، 80 مليون إلكترون فولت من الطاقات الساقطة. إن طبيعة هذه الجهود قد تم تحديدها أولاً باستخدام زوايا الطور المتوفرة ونظرية التشتت العكسي لتحديد أشكالها في منطقة ذيل التوزيع باستخدام معادلة كلاين–جوردن وبعدها تعديل معاملاتها. تأثيرات كولوم تم إدخالها باستخدام توصيف ستركر. هذه الدراسة تؤسس إلى أن الجزء الحقيقي للجهد النووي للبيونات الموجبة والسالبة هو نفسه لهذه الطاقات الثلاث. إنّ نجاح هذه المقاربة، خاصة في منطقة الطاقة المتوسطة، والتي تمثّل منطقة انتقال بين منطقتي الرنين والطاقة المنخفضة جداً، يعطي دافعاً قوياً لتوسيع هذه الدراسة لتشمل طاقات أخرى لـ نواة الكالسيوم ولأهداف نووية أخرى.

Journal of the Association of Arab Universities for Basic and Applied Sciences (2013) **14**, 32–37

University of Bahrain

Journal of the Association of Arab Universities for Basic and Applied Sciences

www.elsevier.com/locate/jaaubas
www.sciencedirect.com

ORIGINAL ARTICLE

Analyses of elastically scattered charged pions from ^{40}Ca in the intermediate-energy region

Zuhair F. Shehadeh *

Physics Department, Taif University, Taif, P.O. Box 888, Saudi Arabia

Received 3 March 2012; revised 24 January 2013; accepted 3 March 2013
Available online 2 April 2013

KEYWORDS

Pion-^{40}Ca potential;
Elastic scattering;
Inverse scattering theory

Abstract The data of differential cross sections for elastically scattered charged pions from ^{40}Ca have been analyzed using a simple local optical potential for 50, 65, and 80 MeV incident energies. The nature of these potentials has been determined first by using the available phase shifts and an inverse scattering theory to determine their forms at the tail region using the Klein–Gordon equation and then adjusting its parameters. The Coulomb effects are incorporated by using Stricker's prescription. The study establishes that the real part of the nuclear potential for π^+ and π^- is the same at these three energies. The success of this approach, especially in this intermediate energy region, which represents a transition region between resonance and very low-energy regions, provides a strong argument for extending this study at other energies for Ca-target and for other nuclear targets.

1. Introduction

Pions are one of the important mesons determining the long range part of the nucleon–nucleon interaction and are key ingredients toward understanding the nature of strong interactions. For this purpose, at least three major dedicated research facilities, Los Alamos Meson Physics Facility (LAMPF), Paul Scherrer Institute/Swiss Institute of Nuclear research (PSI/SIN) and Tri-University Meson Facility (TRIUMF) have been built to study meson-nucleon and meson-nucleus physics. Consequently, many data of high quality on pion-nucleon and pion–nucleus scatterings, in particular pion–nucleus elastic ones, have been taken over the last few decades (Dam et al., 1982; Gretillat et al., 1981; Burleson et al., 1994; Krane, 1988; Preedom et al., 1981; Seth et al., 1990; Shalaby et al., 2007).

The understanding of elastically scattered pions by nuclei forms the first step in determining the many pion–nucleus processes such as inelastic scattering, single charge exchange, double charge exchange, meson productions, . . .etc. (Blecher et al., 1979). The early elastic scattering data on pion-nuclei systems have primarily been taken at the forward angles. The potentials deduced from the analyses of these early data are well summarized in a book (Ericson and Weise, 1988). These early potentials have been only marginally successful in deducing the nature of the pion–nucleus potential as noted by (Leitch et al., 1984) and contradicted the first data taken over the entire angular range for 163.3 MeV pions scattered by ^{40}Ca

* Tel.: +966 531229109.
E-mail address: zfs07@hotmail.com.

Peer review under responsibility of University of Bahrain.

ELSEVIER Production and hosting by Elsevier

1815-3852
http://dx.doi.org/10.1016/j.jaubas.2013.03.003

(Shehadeh et al., 2003). (Satchler, 1992) could, however, provide a reasonable analysis of the data using a simple optical model potential, akin to the one usually used to analyze nucleons scattered by nuclei. He, however, used a modified form of the Klein–Gordon (K–G) equation for the analysis. Similar analyses have been successful to describe elastically scattered pions at other energies incident on calcium (Khallaf and Ibrahim, 2006; Akhter et al., 2001).

The potential deduced by Satchler, however, needed modification when full K–G equation was used (Shehadeh et al., 2003) to describe this process. The determination of this and subsequent potentials by (Shehadeh, 2009) were facilitated by the use of an inverse scattering theory (IST) at a fixed energy developed for the K–G equation (Shehadeh et al., 1999) using the phase shifts extracted primarily from data at forward angles (FrÖhlich et al., 1984). The determined potential is strictly speaking for the scattering of π^0 by ^{40}Ca since the Coulomb interaction was neglected. The first analysis incorporating the Coulomb interaction between π^+ and ^{40}Ca in the K–G equation (Shehadeh et al., 2011) slightly modifies the parameters of the previous. The latter, however, indicated that a simple way to incorporate the Coulomb effect on elastic scattering is to use Stricker's prescription (Stricker et al., 1979) in conjunction with the K–G equation without incorporating explicitly the Coulomb term in the potential function.

In this paper, we extend our studies to 50, 65 and 80 MeV incident energies for both positively and negatively charged pions and ^{40}Ca target. In view of the success of Stricker's prescription noted in the preceding paragraph, the analyses have been carried out using the K–G equation with the Coulomb effect being incorporated using Stricker's prescription. The conversion from laboratory energy to the center of mass has been carried out using Satchler's method. As before, the IST has been used to determine the nature of the potential. As noted later, the points of the potential determined from the IST are suitable in the exterior region and not in the region up to about 3 fm from the center.

The theory, which points a formulation of kinematic parameters and the pion-^{40}Ca potential, is described in Section 2. Section 3 contains the results and their discussions. Section 4 summarizes conclusions.

2. Theory

The radial wave function for the K–G equation for spherically symmetric potential $V(r)$ is determined by the following equation:

$$\left[d^2/dr^2 + k^2 - U(r) - \frac{l(l+1)}{r^2}\right] R_{nl}(r) = 0 \tag{1}$$

where k^2 and $U(r)$ are expressed as:

$$k^2 = (E^2 - m^2c^4)/\hbar^2c^2 \tag{2}$$

$$U(r) = \frac{2E}{\hbar^2c^2}\left[V(r) - V^2(r)/2E\right] = V_{\text{eff}} \tag{3}$$

with $V(r)$ the nuclear part of the potential.

In order to use a non-relativistic optical model computer code, the HARDCORE (Rickertsen et al., 1969), to describe the scattering at relativistic energy, the Satchler's treatment has been used in calculating kinematic parameters. In the treatment, the center-of-mass kinetic energy, $E_{\text{c.m.}}$, is defined as:

$$E_{\text{c.m.}} = \frac{\hbar^2k^2}{2\mu} \tag{4}$$

where $\hbar k$ is the relativistically correct center-of-mass momentum of the pion and μ is the reduced mass of the two interacting particles:

$$\mu = \frac{M_\pi m_T}{M_\pi + m_T} \tag{5}$$

where m_T is the target mass and M_π is the effective mass of the incident pion which is defined as

$$M_\pi = \gamma_\pi m_\pi \tag{6}$$

with $m_\pi c^2 = 139.6$ MeV, and $\gamma_\pi = (x + \gamma_\ell)(1 + 2x\gamma_\ell + x^2)^{-1/2}$ where $x = m_\pi/m_T$ and $\gamma_\ell = 1 + K_\ell/m_\pi c^2$; K_ℓ is the pion bombarding energy in the laboratory system.In (4) k is given by:

$$\begin{aligned} k &= \left(\frac{m_\pi c}{\hbar}\right)\left(\gamma_\pi^2 - 1\right)^{1/2} = \frac{1}{m_\pi}\left(\frac{m_\pi c^2}{\hbar c}\right) m_\pi \left(\gamma_\pi^2 - 1\right)^{1/2} \\ &= 4.72056 m_\pi \left(\gamma_\pi^2 - 1\right) fm^{-1} \end{aligned} \tag{7}$$

In atomic mass units u, one can use $m_\pi = 0.1499u$ and $m_T = 40u$ for ^{40}Ca.With this, one can rewrite (4) as,

$$E_{c.m.} = 20.901 \frac{k^2}{\mu(u)} \text{MeV} \tag{8}$$

Substituting (5) and (7) in (8), $E_{\text{c.m.}}$ can be easily calculated.

It is worth mentioning that M_π and $E_{\text{c.m.}}$ have to be redefined in the code accordingly.

In this investigation, a simple local optical potential has been used. The simplicity and global success of this potential compared to limited successes of other complicated potentials, with deficiencies and drawbacks, require to test its capability, reliability, validity and strength to explain the elastic scattering data of pions of both charges from ^{40}Ca in the low-energy region; namely $T_\pi = 80$, 65, and 50 MeV. At other energies, Satchler's potential $V_s(r)$, given by

$$\begin{aligned} V_s(r) = &\frac{V_o}{1 + \exp\left(\frac{r - R_o}{a_o}\right)} + i\frac{W_2}{1 + \exp\left(\frac{r - R_2}{a_2}\right)} + i \\ &\times \frac{W_3 \exp\left(\frac{r - R_3}{a_3}\right)}{\left[1 + \exp\left(\frac{r - R_3}{a_3}\right)\right]^2} \end{aligned} \tag{9}$$

has to be modified (Shehadeh, 1995) by adding the term

$$V_1(r) = \frac{V_1}{\left[1 + \exp\left(\frac{r - R_1}{a_1}\right)\right]^2} \tag{10}$$

to its real part. Thus the new complex potential used herein is

$$V(r) = V_S(r) + V_1(r) \tag{11}$$

In (3), $V(r)$ is the potential that contains the non-Coulombic part of pion–nucleus interaction.

As noted earlier, Coulomb effects are considered by following Stricker's treatment (Stricker et al., 1979), i.e. by observing the fact the incident kinetic energy near the Coulomb barrier height, defined in (12), is approximately zero for positively charged pions. Hence, the Coulomb effect could approximately be incorporated by lowering the incident kinetic energy by the amount of the barrier height, in this case approximately by 7.6 MeV, for positively charged pions and increasing it by the same amount for negatively charged pions. Thus, the

K–G equation used to treat chargeless pions could be applied to describe the scattering of charged pions by adjusting the incident energy by the Coulomb barrier height energy defined as

$$V_c = \pm \frac{Z_T e^2}{R_c} \tag{12}$$

In (12), $Z_T = 20$ is the target's atomic number, $e^2 = 1.44$ MeV fm, and $R_c = 3.8$ fm is the effective Coulomb radius. The negative and positive signs are for π^+ and π^-, respectively. As such, and for $\pi^{\pm}$–^{40}Ca cases, V_c is approximately 7.6 MeV. The incident kinetic energy is, then, modified by V_c to reflect the Coulomb effect.

Table 1 The parameters of the imaginary potential W_2 (in MeV), R_2 (in fm), a_2 (in fm), W_3 (in MeV), R_3 (in fm), and a_3 (in fm), used in Eq. (11) for the incident-energy charged pions (T_π in MeV). Positive and negative signs in the first column indicate π^+ and π^-, respectively.

T_π	W_2	R_2	a_2	W_3	R_3	a_3
80(+)	380	2.821	0.135	211.6	2.487	0.720
80(−)	50		0.245	111.6		
65(+)	100	3.121	0.135	211.6	1.887	0.720
65(−)	40	3.321			1.387	0.900
50(+)	200	2.750	0.175	111.6	1.387	0.900
50(−)	55	3.100	0.155			0.700

3. Results and discussion

The starting point of this investigation is the use of IST, outlined in appendix A, to determine the points of the potential in the exterior region. As pointed by (Alam and Malik, 1991) and references therein, the points determined in the interior region i.e., $r < 3$ fm, are uncertain.

Using the potential points obtained from the inverse scattering theory as a guide, I, therefore construct the potential by adjusting the parameters of the real part of the potential and obtain $V_0 = 24.5$ MeV, $R_0 = 5.119$ fm, $a_0 = 0.153$ fm, $V_1 = 120$ MeV, $R_1 = 1.22$ fm, and $a_1 = 0.663$ fm. Benefitting from a previous study (Shehadeh, 2009), these parameters were kept fixed.

On the other hand, the parameters of the imaginary part are changed according to potential points extracted from IST to provide reasonable fits to the observed angular distributions. These parameters are listed in table 1. In the interior region, generally for $r \leqslant 3fm$, points determined using IST are usually uncertain. This is further complicated by the fact that Fröhlich et al. have done the phase shift analyses using forward angle data only which could make the determined phase shifts somewhat uncertain.

On the left side of Fig. 1, the calculated angular distributions in the 80 MeV case, obtained by neglecting the squared potential term, $V^2/2E$, in (3) (upper insert) and including it (lower insert) in (11) are compared with the observed data (Leitch et al., 1984). In the same figure (right side), the analytical potential forms joining the points of the real and imaginary parts of

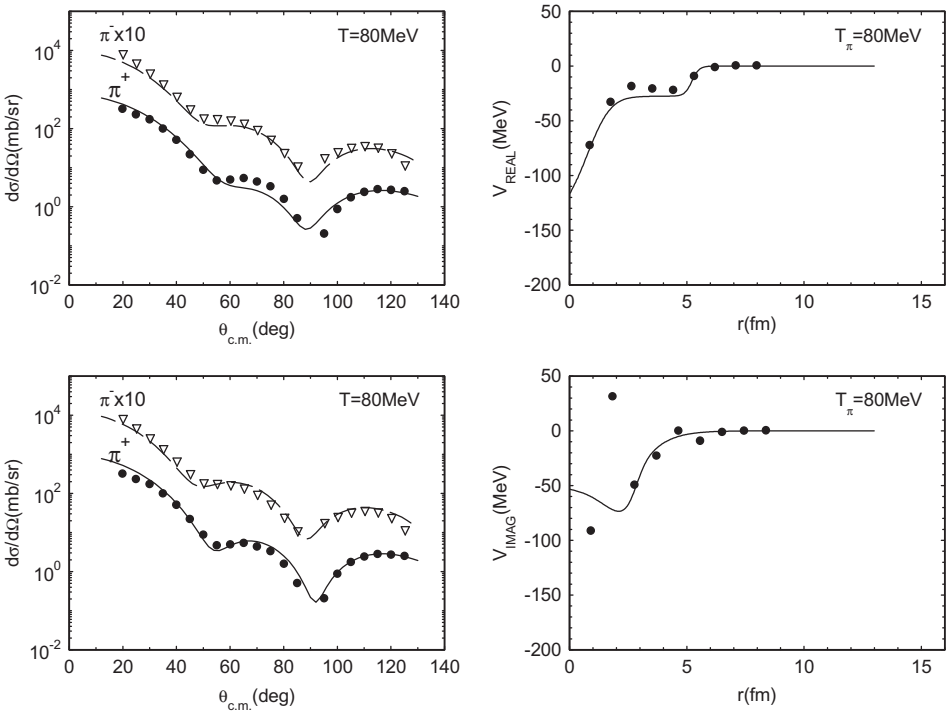

Figure 1 On the left side, the calculated angular distributions (solid and dashed lines) using the potential given by Eq. (11) without the squared potential, $V^2/2E$, in (3) (upper part) and with including it (lower part) are compared with the experimental data (solid circles and empty triangles) reported by Leitch et al. (1984) as a function of center of mass angle ($\theta_{c.m.}$) for $T_\pi = 80$ MeV for positively and negatively charged pions, respectively. On the right side, the real and imaginary parts of the potential given by Eq. (11), with the squared potential term included, are compared with the potential points obtained by using the inverse scattering theory for positive pions.

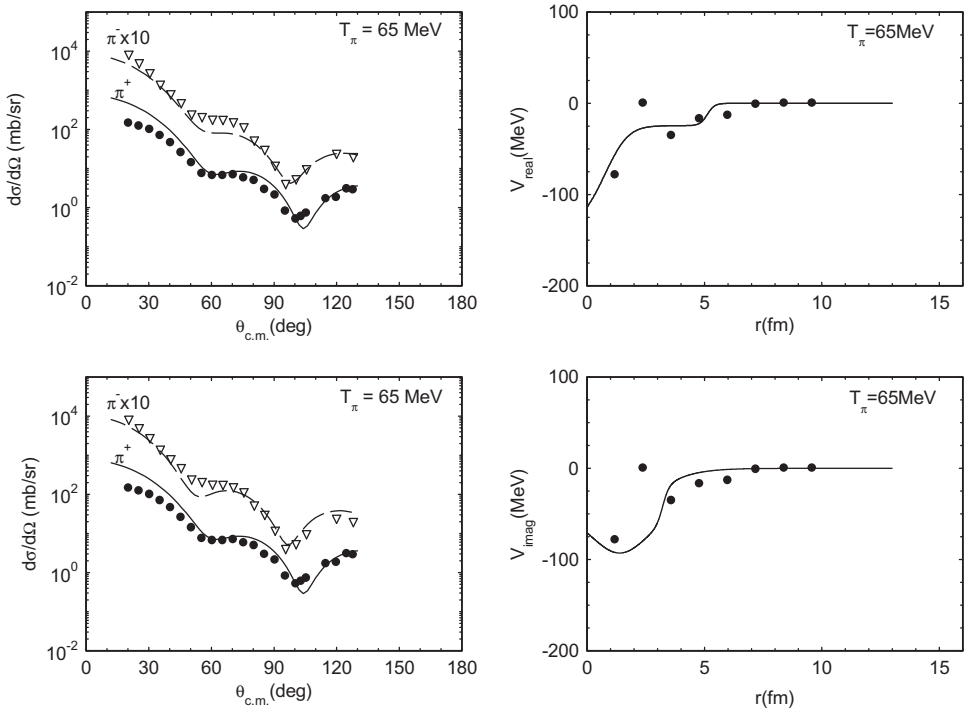

Figure 2 Same as Fig. 1 but for the 65 MeV case.

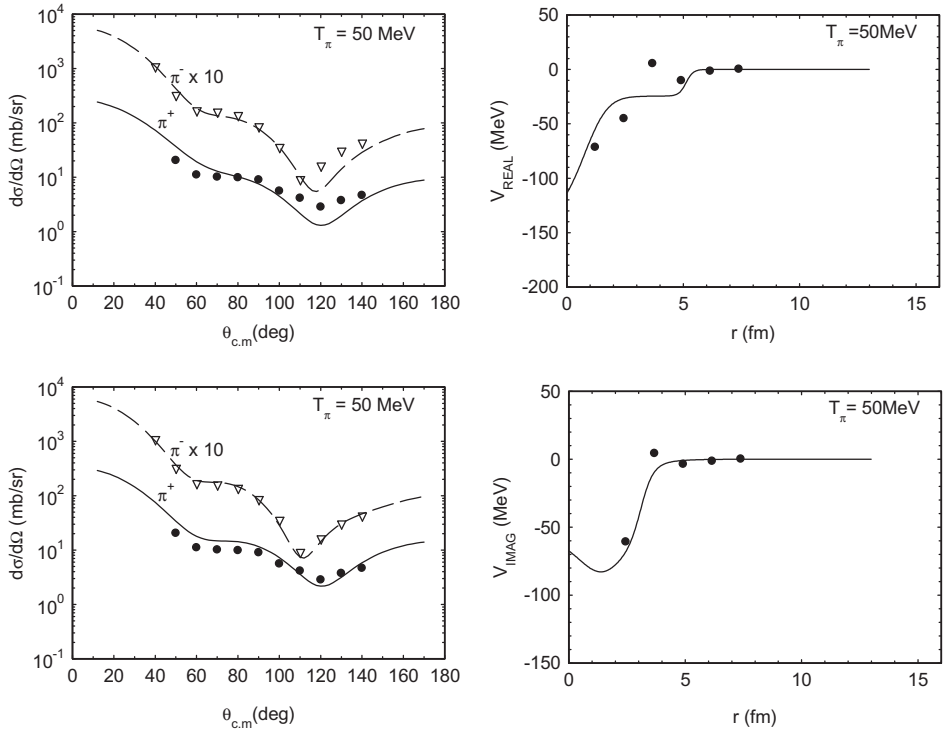

Figure 3 Same as Fig. 1 but for the 50 MeV case.

the effective potential, defined by (A.4) and (A.5), respectively, are shown by solid lines. Similar graphs are shown in Figs. 2 and 3 for 65 and 50 MeV incident $\pi^{\pm}$. The data are from (Dam et al., 1982; Fröhlich et al., 1984), respectively. The inclusion of the squared potential term in the potential (11) improves the fits for both positive and negative pions. Therefore, its inclusion in studying data at higher energies is warranted. From these graphs, it is very clear that the points of the potential obtained from the IST serve very well in determining the nature of the potential from a distance of 3 fm outward. This success is a

strong motivation for initiating a comprehensive study of determining potentials from the elastically scattered charged pions from ^{40}Ca at all energies where phase shift analyses are available. In addition, this work will be extended to treat the scattered charged pions from other nuclei, such as ^{16}O and ^{12}C, at energies where phase shift analyses are available (Fröhlich et al., 1981; Dumbrajs et al., 1984).

4. Conclusions

This analysis establishes a number of very important points illuminating the nature of pion–nucleus potential, the most important of them being that the non-Coulomb real part of the pion–nucleus potential is the same for π^+ and π^- at incident energies considered herein. The others are the following: (a) The analyses of large angle data require the inclusion of $V^2(r)$ term in the K–G equation which often is omitted. (b) The potential points determined from about 3 fm outward can be reasonably obtained by the IST and (c) As already noted by Shehadeh et al. (2011), Stricker's prescription is a reasonable way to incorporate the effect of the Coulomb term.

5. Appendix A

It is well-known that pion–nucleus interaction is governed by the Klein–Gordon equation with a spherically symmetric potential, $V(r)$, that can be written as:

$$\left[d^2/dr^2 + k^2 - U(r) - \frac{l(l+1)}{r^2}\right] R_{nl}(r) = 0 \tag{A.1}$$

where $R_{nl}(r)$ is the r times the radial part of the wave function for a spherical symmetric external potential. Also, in (1), k^2 and $U(r)$ are given by

$$k^2 = \left(E^2 - m^2c^4\right)/\hbar^2c^2 \tag{A.2}$$

$$U(r) = \frac{2E}{\hbar^2c^2}\left[V(r) - V^2(r)/2E\right] = V_{eff} \tag{A.3}$$

In (A.3), E and m are, respectively, total energy and pion rest mass and c is the velocity of electro-magnetic wave in vacuum. $V(r)$ is the complex pion–nucleus potential.

Since $V(r)$ is complex, the real and imaginary part of the effective potential, ReU and ImU, respectively, have the following expressions:

$$\mathrm{Re}U(r) = \left(\frac{2E}{\hbar^2c^2}\right)\left[\mathrm{Re}V(r) - \frac{\{(\mathrm{Re}V(r))^2 - (\mathrm{Im}V(r))^2\}}{2E}\right] \tag{A.4}$$

$$\mathrm{Im}U(r) = \left(\frac{2E}{\hbar^2c^2}\right)\left[\mathrm{Im}V(r) - \frac{2(\mathrm{Re}V(r))^2 - (\mathrm{Im}V(r))^2}{2E}\right] \tag{A.5}$$

For completeness and importance, the inverse scattering theory used to extract the real and imaginary parts of the effective potential (Shehadeh et al., 1995) is summarized in the following. Introducing

$$\varphi_{nl}(r) = (kr)^{-(l+1)} R_{nl}(r) \tag{A.6}$$

one obtains the following equation for $\varphi_{nl}(r)$ from (A.1),

$$\left[\frac{d^2}{dr^2} + \frac{2(l+1)}{r}\frac{d}{dr} + k^2 - U(r)\right]\varphi_{nl}(r) = 0 \tag{A.7}$$

Dividing the range, R, of $U(r)$ in N equal parts, one has $R = N\Delta$ and the point $r = n\Delta$ with n being an integer. Replacing the differential operators by central differences, one may obtain from (A.7) the following difference equation

$$\varphi_{n+1} = A_n(l)B_n(l)\varphi_n + C_n(l)\varphi_{n-1}; n = 1, 2...N \tag{A.8}$$

In (A.8), we have suppressed the suffice (nl) in φ and $A_n(l)$, $B_n(l)$ and $C_n(l)$ are given by the following expressions:

$$A_n(l) = 2 - \Delta^2k^2 + \Delta^2U_n \tag{A.9}$$

$$B_n(l) = n/(l+1+n) \tag{A.10}$$

$$C_n(l) = (l+1-n)/(l+1+n) \tag{A.11}$$

and U_n is the value of U at the n-th point. The logarithmic derivative relevant for the calculation of phase shifts for a given l, $Z_N(l)$ is given by replacing the first derivative by central difference at $R = N\Delta$, and is the following:

$$Z_N(l) = \left(\frac{N}{2}\right)\left(\frac{\varphi_{N+1} - \varphi_{N-1}}{\phi_N}\right) \tag{A.12}$$

The evaluation of (A.12) requires the knowledge of φ_N, φ_{N+1} and φ_{N-1} at $n = N$. For $n = N$, (A.8) reduces to

$$\frac{\varphi_{N+1}}{\varphi_N} = A_N(l)B_N(l) + C_N(l)/(\varphi_N/\varphi_{N-1}) \tag{A.13}$$

One may now replace $(\varphi_N/\varphi_{N-1})$; successively and obtain the following continued fraction equation

$$\frac{\phi_{N+1}}{\varphi_N} = A_N(l)B_N(l) + \left[\frac{C_N(l)}{A_{N-1}(l)B_{N-1}(l)+}\frac{C_{N-1}(l)}{A_{N-2}(l)B_{N-2}(l)+}\ldots \frac{C_3(l)}{A_2(l)B_2(l)+}\frac{C_2(l)}{A_1(l)B_1(l) + C_1(l)/(\varphi_1/\varphi_0)}\right] \tag{A.14}$$

Since for a given l, there is always a point "m" where $C_m(l) = 0$, the last term in the continued fraction does not enter in the calculation. One can similarly calculate φ_{N-1}/φ_N and obtain $Z_N(l)$ and hence, the phase shift.

For the inverse scattering process, one starts at a point where $U_N = 0$. At that point $A_N = 2-\Delta^2k^2$, is known. Using (A.12) and (A.13) at that point one gets

$$\frac{\varphi_N}{\varphi_{N-1}} = \frac{C_N(l)}{\left[\frac{2}{N}Z_N(l) - A_N(l)B_N(l)\right]} \tag{A.15}$$

where $l = 0,1,2\ldots,L$ and $N = L + 1$, L being the largest partial wave. As noted earlier, there is always an l_n that makes $C_n(l_{N-n}) = 0$. For $n = N-1$, we therefore, have

$$A_{N-1}(l_1) = \frac{1}{B_{N-1}(l_1)}\frac{\varphi_N(l_1)}{\varphi_{N-1}(l_1)} \tag{A.16}$$

This inward iteration may be continued to find all A_{N-j} at the points for $j = 2,3\ldots N-1$

$$A_{N-j}(l_j) = \frac{1}{B_{N-j}(l_j)}\left[\frac{C_{N+1-j}(l_j)}{-A_{N+1-j}(l_j)B_{N+1-j}(l_j)+}\ldots\frac{C_{N-2}(l_j)}{-A_{N-2}(l_j)B_{N-2}(l_j)+} \cdot\frac{C_{N-1}(l_j)}{-A_{N-1}(l_j)B_{N-1}(l_j) + \varphi_N(l_j)/\varphi_{N-1}(l_j)}\right] \tag{A.17}$$

Once $A_{N-j}(l_j)$ is known, U_n is given by

$$U_n = \frac{1}{\Delta^2}\left[A_n - 2 + \Delta^2k^2\right] \tag{A.18}$$

and hence, both the real and imaginary parts at points $n = N-1$ of V_{eff} can be calculated.

Acknowledgments

The author thanks Prof. F.B. Malik for fruitful discussions and careful reading of the manuscript. Also, the author is very pleased to acknowledge the financial support of the Deanship of Scientific Research at the Taif University, Taif, Saudi Arabia for this investigation.

References

Akhter, M.D.A.E., Sultana, S.A., Sen Gupta, H.M., Peterson, R.J., 2001. Local optical model studies of pion–nucleus scattering. J. Phys. G: Nucl. Part. Phys. 27, 755–771.

Alam, M.M., Malik, F.B., 1991. An inverse scattering method for identical particles. Nucl. Phys. A 524, 88–94.

Blecher, M., Gotow, K., Jenkins, D., Milder, F., Bertrand, F.E., Cleary, T.P., Gross, E.E., Ludemann, C.A., Moinester, M.A., Burman, R.L., Hamm, M., Redwine, R.P., Yates-Williams, M., Dam, S., Darden III, C.W., Edge, R.D., Malbrough, D.J., Marks, T., Preedom, B.M., 1979. Positive pion–nucleus elastic scattering at 40 MeV. Phys. Rev. C 20, 1884–1890.

Burleson, G., Blanpied, G., Cottigame, W., Daw, G., Park, B., Seth, K.K., Barlow, D., Iversen, S., Kaletka, M., Nann, H., Saha, A., Smith, D., Redwine, R.P., Burger, W., Farkhondeh, M., Sanghai, B., Anderson, R., 1994. Negative pion–nucleus elastic scattering at 20 and 40 MeV. Phys. Rev. C 49, 2226–2229.

Dam, S.H., Edge, R.D., Preedom, B.M., Hamm, M., Burman, R.L., Carlini, R., Redwine, R.P., Yates, M.A., Blecher, M., Gotow, K., Bertrand, F.E., Gross, E.E., Moinester, M.A., 1982. Elastic Scattering of π^+ and π^- for ^{40}Ca at 64.8 MeV. Phys. Rev. C 25, 2574–2581.

Dumbrajs, O., Fröhlich, J., Klein, U., Schlaile, H.G., 1984. Analysis of $\pi^{\pm}$–^{12}C elastic scattering. Phys. Rev. C 29, 581–591.

Ericson, T., Weise, W., 1988. Pions and Nuclei. Clarendon Press, Oxford, England.

Fröhlich, J., Schlaile, H.G., Streit, L., Zingl, H., 1981. An improvement of coulomb corrections in the phase shift analysis of elastic $\pi^{\pm}$–^{16}O scattering and predictions of cross sections for π^-–^{16}O scattering at low energies. Z. Phys. A 302, 89–94.

Fröhlich, J., Pilkuhn, H., Schlaile, H.G., 1984. Phase-shift analysis of elastic $\pi^{\pm}$–^{40}Ca scattering between 0 and 300 MeV. Nucl. Phys. A 415, 399–412.

Gretillat, P., Egger, J.P., Germond, J.F., Lunke, C., Schwarz, Perrin, E.C., Preedom, B.M., 1981. Study of π^+ and π^- elastic scattering from ^{40}Ca and ^{48}Ca in the region of πN (3,3) resonance. Nucl. Phys. A 364, 270–284.

Khallaf, S.A., Ibrahim, A.A., 2006. Phenomenological local potential analysis of π^+ scattering. FIZIK B 14, 333–348.

Krane, K.S., 1988. Introductory Nuclear Physics. John Wiley & Sons, New York, United States.

Leitch, M.J., Burman, R.L., Carlini, R., Dam, S., Sandberg, V., Blecher, M., Gotow, K., Ng, R., Auble, R., Bertrand, F.E., Gross, E.E., Obenshain, F.E., Wu, J., Blanpied, G.S., Preedom, B.M., Ritchie, B.G., Bertozzi, W., Hynes, M.V., Kovash, M.A., Redwine, R.P., 1984. Pion–nucleus elastic scattering at 80 MeV. Phys. Rev. C 29, 561–568.

Preedom, B.M., Dam, S.H., Darden III, C.W., Edge, R.D., Malbrough, D.J., Marks, T., Burman, R.L., Hamm, M., Moinester, M.A., Redwine, R.P., Yates, M.A., Bertrand, F.E., Cleary, T.P., Gross, E.E., Hill, N.W., Ludemann, C.A., Blecher, M., Gotow, K., Jenkins, D., Milder, F., 1981. Positive pion–nucleus elastic scattering at 30 and 50 MeV. Phys. Rev. C 23, 1134–1140.

Rickertsen, L., Block, B., Clark, J., Malik, F.B., 1969. Nuclear heavy-ion heavy-ion collisions and the intermediate state model. Phys. Rev. Lett. 22, 951–955.

Satchler, G.R., 1992. Local potential model for pion–nucleus scattering and π^+/π^- excitation ratios. Nucl. Phys. A 540, 533–576.

Seth, K., Barlow, D., Iverson, S., Kaletka, M., Nann, H., Smith, D., Artuso, M., Burleson, G., Blanpied, G., Daw, G., Burger, W., Redwine, R., Saghai, B., Anderson, R., 1990. Negative pion–nucleus elastic scattering at 30 and 50 MeV. Phys. Rev. C 41, 2800–2808.

Shalaby, A.S., Hassan, M.Y.M., El-Gogary, M.M.H., 2007. Multiple scattering theory for pion–nucleus elastic scattering and the in-medium πN amplitude. Br. J. Phys. 37, 388–397.

Shehadeh, Z.F., 2009. Analysis of pion-^{40}Ca elastic scattering data using the Klein–Gordon equation. Int. J. Mod. Phys. E 18, 1615–1627.

Shehadeh, Z.F., 1995. Non-Relativistic Nucleus–Nucleus and Relativistic Pion–Nucleus Interactions, Ph.D. Thesis, Southern Illinois University at Carbondale, Illinois, USA.

Shehadeh, Z.F., Alam, M.M., Malik, F.B., 1999. Inverse scattering theory at a fixed energy for the Klein–Gordon equation. Phys. Rev. C 59, 826–831.

Shehadeh, Z.F., Sabra, M.S., Malik, F.B., 2003. Pion-^{40}Ca Potential using inverse scattering formalism and the Klein–Gordon equation. Condens. Matter Theor. 18, 339–346.

Shehadeh, Z.F., Scott, J.S., Malik, F.B., 2011. Analysis of 2009. Analysis of $\pi^{\pm}$–^{40}Ca elastic scattering data in the delta resonance region using inverse scattering theory and the Klein–Gordon equation. AIP Conf. Proc. 1370, 185–191.

Stricker, K.S., 1979. A Study of the Pion–Nucleus Optical Potential, Ph.D. Thesis, Michigan State University, Michigan, USA.